JPE 2-2-9

A High-Performance Sensorless Control System of Reluctance Synchronous Motor with Direct Torque Control by Consideration of Nonlinearly Inductances

Min-Huei Kim*, [1]Nam-Hun Kim, and [1]Won-Sik Baik

Dept. of Electrical Automatic Eng., Yeungnam college of Science & Technology, Daegu, Korea
[1]School of Electrical and Electronic Eng., Yeungnam University, Kyeungsan, Korea

ABSTRACT

This paper presents an implementation of digital control system of speed sensorless for Reluctance Synchronous Motor (RSM) drives with direct torque control (DTC). The problem of DTC for high-dynamic performance RSM drive is generating a nonlinear torque due to a saturated nonlinear inductance curve with various load currents. The control system consists of stator flux observer, compensating inductance look-up table, rotor position/speed/torque estimator, two hysteresis band controllers, an optimal switching look-up table, IGBT voltage source inverter, and TMS320C31 DSP controller. The stator flux observer is based on the combined voltage and current model with stator flux feedback adaptive control that inputs are the compensated inductances, current and voltage sensing of motor terminal with estimated rotor angle for wide speed range. The rotor position is estimated by observed stator flux-linkage space vector. The estimated rotor speed is determined by differentiation of the rotor position used only in the current model part of the flux observer for a low speed operating area. It does not require the knowledge of any motor parameters, nor particular care for motor starting, In order to prove the suggested control algorithm, we have simulation and testing at actual experimental system. The developed sensorless control system is showing a good speed control response characteristic results and high performance features in 20/1500 rpm with 1.0Kw RSM having 2.57 ratio of d/q reluctance.

Key Words: RSM, Speed Sensorless, Stator Flux Observer, DTC, Inductance Compensator

1. Introduction

In recent years, a motion control system with high dynamic performance and accuracy is necessary in industrial application field. A vector control system for motor drives have been widely used because of their advantage such as simplicity, rugged structure, reliability, high maintainability and economy.

However, the vector control techniques incorporating fast microprocessor and digital signal processing (DSP) have made possible the application of motor drive system using a position/speed sensor for high-performance system due to sophisticated and large computational time. In order to solve this problem, many researchers have been developed to find out different solutions for motor control system having features of precise and quick torque response, and reduction of the complexity of vector control algorithms [1-14].

Manuscript received January 8, 2002; revised April 28, 2002.

Corresponding Author: mhkim@ync.ac.kr, Tel: +82-53-650-9263. Fax: +82-53-624-4736

The direct torque control (DTC) recognized as viable solution to achieve these requirements. In principle the DTC selects one of the six voltage vectors and two zero voltage vectors generated by voltage source inverter to keep stator flux and torque within the limits of two hysteresis band. This method uses direct control the stator flux and torque without using current regulator, sophisticated estimation, PI control of flux and torque, which are proposed to decrease the parameter sensibility problem characterizing the vector algorithms [1-5].

The synchronous reluctance motors(RSM) have recently attracted as a viable alternative to induction, synchronous and switched reluctance machines in medium-performance drive applications. This has been made possible by limiting some traditional RSM drawbacks, such as poor power factor and low-torque density, related to the limited saliency ratio obtainable using conventional rotor design. Its stator has windings similar to those of a three-phase induction motor and a rotor designed with appreciably different values of the reluctance on the direct and quadrature axes. The RSM has the advantages of both the induction motor and the permanent magnet motor. Because of their inherent simplicity and ruggedness, RSM can be used in many industrial and automotive applications [6-7].

Unfortunately, RSM is disadvantaged as it needs a suitable position sensor in order to synchronize the stator current vector with the rotor position. Since position sensor increase costs, sizes, and circuit complexity of motor drives, while often reducing their reliability, position/speed sensorless control system for motor drives have been recently proposed where estimation of the actual rotor position/speed is obtained by motor terminal current and voltage measurement[8-9]. The accurate estimation of the stator flux and torque with various load current can obtained by using a saturated inductance compensator from measuring the modulus and angle of the stator current space vector [8, 14].

In the present paper, an implementation of digital sensorless speed control system for RSM drives with direct torque control using inductance compensator is proposed. The suggested sensorless control algorithm is showing a good speed control response and high-performance features in 20/1500 rpm with 1.0 kW RSM having 2.57 ratio of d/q reluctance.

2. Direct Torque Control for RSM

2.1 Concept of DTC

A DTC algorithm is possible to control directly by the stator flux linkage and the electromagnetic torque by the selection of optimum inverter switching pattern. The selection is made to restrict the flux and torque errors within respective flux and torque hysteresis bands, to obtain fast torque response, low switching frequency, and low harmonic losses. So that DTC allow very fast torque response and flexible control of RSM. The main advantages of the DTC are the absence of coordinate transformations and voltage decoupling block, reduced number of controller and the effect of motor parameter variation, actual flux-linkage vector position does not have to be determine, but only the sector where the flux linkage is located [7-10].

2.2 Inductance Compensator

The problem of DTC for high-dynamic performance and maximum efficiency RSM drive is generating a nonlinear electromagnetic torque due to a saturated stator linkage flux and nonlinear inductance curve with various load currents. The accurate estimation of the stator flux and torque can be calculated by using a saturated inductance compensator from measuring the modulus and angle of the stator current space vector. Fig. 1 is showing the measured inductance Ld and Lq according to stator current in actual operating system[9, 14]. The inductance compensator with various load current can be made by compensating inductance look-up table from the figure 1.

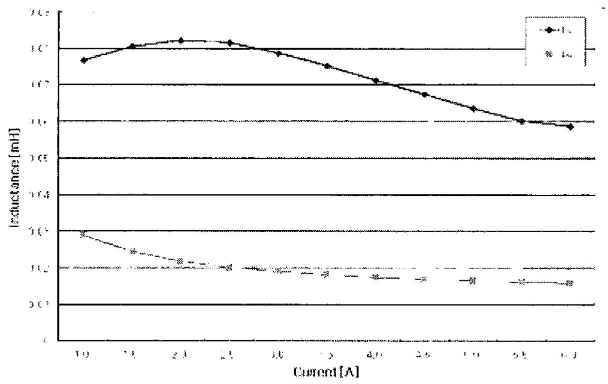

Fig. 1. Measured inductance Ld and Lq according to load current.

2.3 Flux, Torque and Speed Observer

The core of DTC is the control of the amplitude and rotating speed of stator flux linkage. The calculation of stator flux is then very important. One of the best and simplest calculation methods is to calculate the stator flux from stator current, voltage and estimated rotor angle, which is good character in wide speed area[9]. Fig. 2 shows such a closed-loop, stationary frame, observer, which is hereafter described as the "closed-loop flux observer". A closed-loop flux observer is globally stable in the stationary frame and does work at wide speed[11]. The stator flux-linkage in the stator reference frame is Eq. (5). The electromagnetic torque (Te) can be calculated by the observed stator flux-linkage space vector and the measured terminal currents, estimated from Eq. (6).

$$\begin{bmatrix} I^s_{dr} \\ I^s_{qr} \end{bmatrix} = \begin{bmatrix} \cos\theta_r & \sin\theta_r \\ -\sin\theta_r & \cos\theta_r \end{bmatrix} \begin{bmatrix} I^s_{ds} \\ I^s_{qs} \end{bmatrix} \tag{1}$$

$$\begin{bmatrix} \Phi^s_{dr} \\ \Phi^s_{qr} \end{bmatrix} = \begin{bmatrix} I^s_{dr} \cdot Ld \\ I^s_{qr} \cdot Lq \end{bmatrix} \tag{2}$$

$$\begin{bmatrix} \Phi^s_{ds} \\ \Phi^s_{qs} \end{bmatrix} = \begin{bmatrix} \cos\theta_r & \sin\theta_r \\ -\sin\theta_r & \cos\theta_r \end{bmatrix} \begin{bmatrix} \Phi^s_{dr} \\ \Phi^s_{qr} \end{bmatrix} \tag{3}$$

$$\varepsilon_\Phi = \Phi^s_{dqs} - \Phi^{s*}_{dqs} \tag{4}$$

$$\Phi *^s_{dqs} = \int [(V^s_{dqs} - R_s \cdot I^s_{dqs}) + \varepsilon_\Phi (K_1 + \frac{K_2}{P})]dt \tag{5}$$

$$T_e = \left(\frac{3}{2}\right) \left(\frac{P}{2}\right) \left(\Phi^s_{ds} I^s_{qs} - \Phi^s_{qs} I^s_{ds}\right) \tag{6}$$

where, I^s_{dqs} represent stator current, I^s_{dqr} represent rotor current, $\Phi *^s_{dqs}$ represent stator flux-linkage, Φ^s_{dqs} represent stator flux-linkage from current mode, Φ^s_{dqr} represent rotor flux-linkage.

Based on this system, a sensorless DTC drive has been construction. Fig. 3 shows speed and torque estimator. The speed of the stator flux space vector and rotor can be estimated from Eq. (7) and (8). A digital low pass filter used to compute the speed of the stator flux space vector.

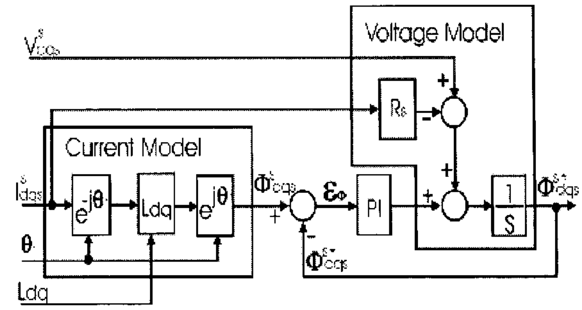

Fig. 2. Stator Flux Observer using compensated Ldq.

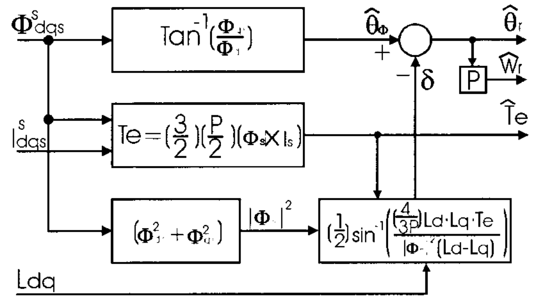

Fig. 3. Position, Speed and Torque Estimator.

An Eq. (9) represents the angle between the stator and rotor flux linkage space vector.

$$\hat{\theta}_\Phi = \tan^{-1}(\Phi_{qs} / \Phi_{ds}) \tag{7}$$

$$\hat{\omega}_r = \frac{d(\hat{\theta}_\Phi - \delta)}{dt} \tag{8}$$

$$\delta = \frac{1}{2}\sin^{-1}(\frac{4 \cdot L_d \cdot L_q \cdot Te}{3P \cdot |\Phi^2| \cdot (L_d - L_q)}) \tag{9}$$

2.4 Optimal switching vector

The DTC algorithm selects optimal switching voltage vector from a look-up table, based on the actual flux and torque value. Those voltage vector construct six non-zero active switching vectors and two zero switching vectors[8]. If a stator flux increase is required then $d\Phi = 1$, if a stator flux decrease is required then $d\Phi = 0$, the digital output signal of two-level hysteresis comparator are determined Eq. (10). If a torque increase is required then dTe=1, if a torque decrease is required them dTe=-1, and if a torque is not change then dTe=0, the digital output signal of three-level hysteresis comparator are determined Eq. (11)

Table 1. Optimal voltage switching vector look-up table.

$\Delta\Phi_e$	ΔT_e	Sect. 1	Sect. 2	Sect. 3	Sect. 4	Sect. 5	Sect. 6
1	1	$\overline{V}_2$	$\overline{V}_3$	$\overline{V}_4$	$\overline{V}_5$	$\overline{V}_6$	$\overline{V}_1$
	0	$\overline{V}_7$	$\overline{V}_0$	$\overline{V}_7$	$\overline{V}_0$	$\overline{V}_7$	$\overline{V}_0$
	-1	$\overline{V}_6$	$\overline{V}_1$	$\overline{V}_2$	$\overline{V}_3$	$\overline{V}_4$	$\overline{V}_5$
0	1	$\overline{V}_3$	$\overline{V}_4$	$\overline{V}_5$	$\overline{V}_6$	$\overline{V}_1$	$\overline{V}_2$
	0	$\overline{V}_0$	$\overline{V}_7$	$\overline{V}_0$	$\overline{V}_7$	$\overline{V}_0$	$\overline{V}_7$
	-1	$\overline{V}_5$	$\overline{V}_6$	$\overline{V}_1$	$\overline{V}_2$	$\overline{V}_3$	$\overline{V}_4$

and Eq. (12) [4, 5, 8]. The optimal switching look-up table shows the Table 1[4, 8, 14].

$$d\Phi = 1, \quad if \quad |\overline{\Phi}_s| \le |\overline{\Phi}_s^*| - |\Delta\overline{\Phi}_s|$$

$$d\Phi = 0, \quad if \quad |\overline{\Phi}_s| \ge |\overline{\Phi}_s^*| - |\Delta\overline{\Phi}_s| \qquad (10)$$

$$dTe = 1, \quad if \quad |T_e| \le |Te_e^*| - |\Delta T_e|$$

$$dT_e = 0, \quad if \quad |T_e| \ge T_e^* \qquad (11)$$

$$dT_e = -1, \quad if \quad |T_e| \ge |T_e^*| + |\Delta T_e|$$

$$dT_e = 0, \quad if \quad T_e \le T_e^* \qquad (12)$$

3. System Configuration

Fig. 4 is shown the proposed speed sensorless control system of RSM with DTC. The control system consists of stator flux observer, compensating inductance look-up table, rotor position/speed estimator, torque estimator, two hysteresis band controllers, an optimal switching look-up table, IGBT voltage source inverter, and TMS320C31 DSP controller by using fully integrated control software. Table 2 are shown the applied RSM parameters

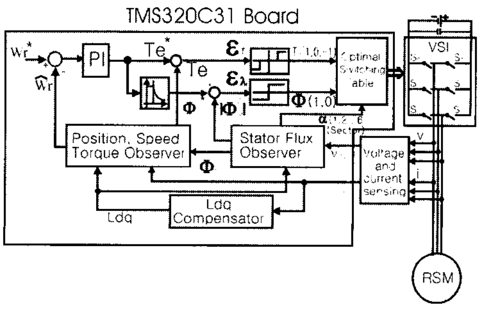

Fig. 4. Proposed Sensorless Control System of RSM.

Table 2. Applied RSM Parameters.

Inertia moment	$0.003[\mathrm{Kg}.m^2]$	Rs	1.0[ohm]
Poles of stator	4	Rated torque	4.0[Nm]
Poles of rotor	4	Reted current	5.0[A]
Rated output	1000[W]	Lq	28[mH]
Rated rpm	2400[rpm]	Ld	72[mH]

4. Simulation Results

Simulation in the SIMULINK environment has been carried out for the evaluation of a proposed control system. In order to show some speed response and high performance characteristics, we carried out some simulations in both low speed range and high-speed range.

Fig. 5 shows the simulation results for the speed control response during 10 seconds with a rotor speed ±50[rpm]. Fig. 5 (a) represents speed response characteristics, (b) torque response, (c) stator flux waveform in transitent state, and (d) locus of stator flux.

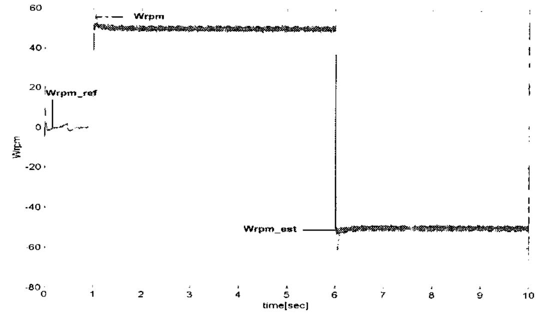

(a) Speed response charecteristics (0 - +50 - -50 rpm)

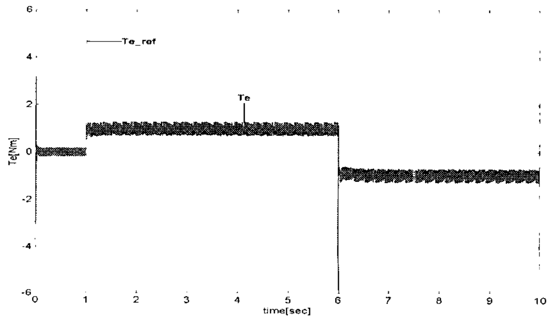

(b) Torque response characteristics

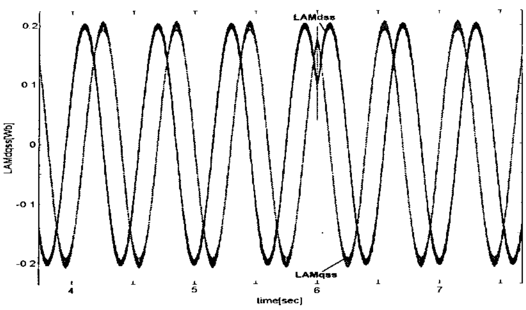

(c) Stator flux waveform in transitent state

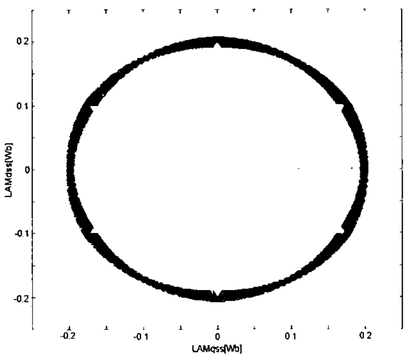

(d) Locus of stator flux

Fig. 5. Simulation results at ±50 [rpm].

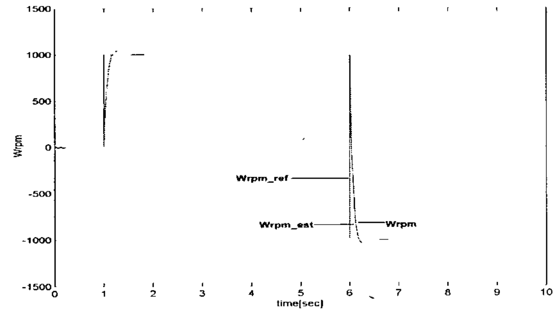

(a) Speed response characteristics (0 - +1000 - -1000rpm)

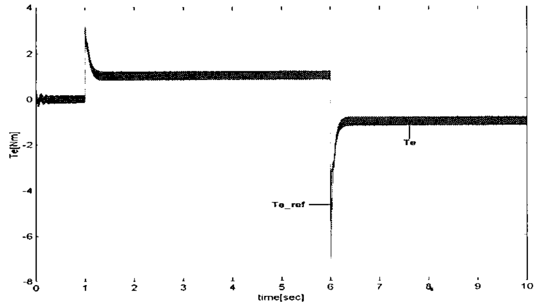

(b) Torque response characteristics

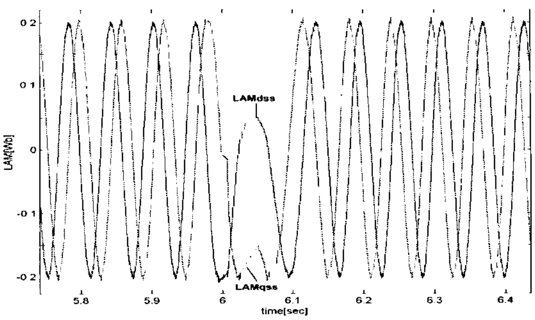

(c) Stator flux waveform in transient state

Fig. 6. Simulation results at ±1000 [rpm].

Fig. 6 shows the simulation results for the speed control response during 10 seconds with a rotor speed ± 1500[rpm]. Fig. 6 (a) represents speed response characteristics, (b) torque response, and (c) stator flux waveform in transitent state.

5. Experimental Results

In order to investigate the experimental validation of the proposed the control system with a DSP based has been used, the experimental set-up includes a fully digital controlled IGBT inverter and 1 kW RSM, which having 2.57 ratio of reluctance values (Ld/Lq). The control scheme has been implemented on a 60MHz TMS320C31 DSP. Table 3 is shown the applied system parameters.

Fig. 7 shows the experimental results for the response of speed control during 10 seconds with a rotor speed ± 20 [rpm]. Fig. 7(a) represents speed response characteristics, (b) torque response, (c) stator flux waveform in transitent state, (d) locus of stator flux and (e) stator current waveform.

Table 3. Applied system parameters.

Current sampling time	0.1[msec]
Theta estimation time	0.1[msec]
Speed estimation time	1.0[msec]
Torque Hys. Band	0.05*Te_ref
Flux Hys. Band	0.05*Flux_ref
Stator Flux Observer	Ki=8.0, Kp=15.0
Speed Controller	Ki=2.5, Kp=0.25

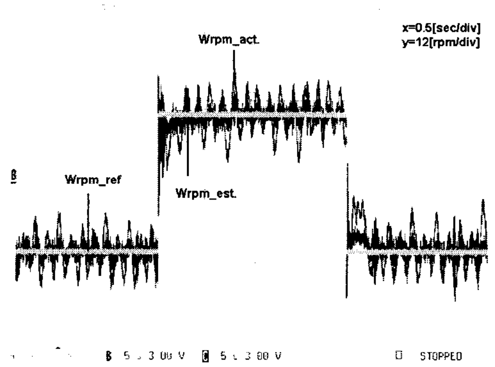

(a) Speed response characteristics(-20 - +20 - -20)

(b) Torque response characteristics

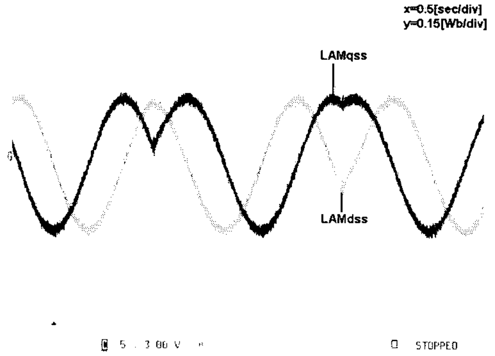

(c) Stator flux waveform in transient state

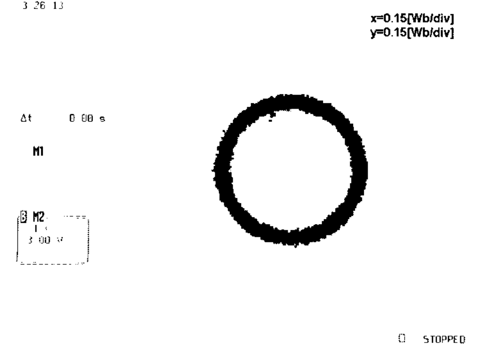

(d) Locus of stator flux

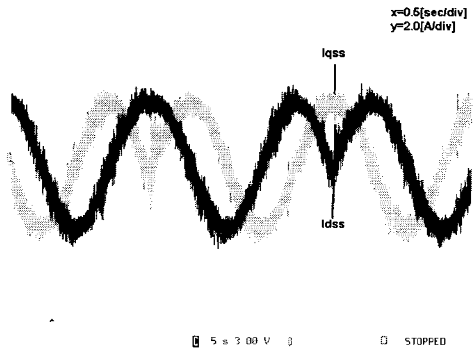

(e) Stator current waveform in transient state

Fig. 7. Experimental results at ±20 [rpm].

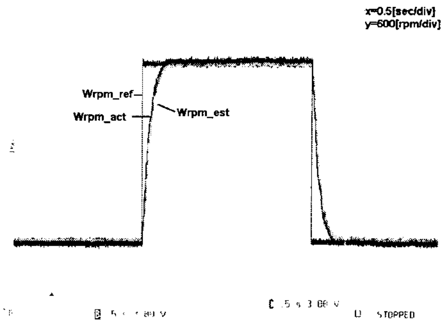

(a) Speed response characteristics

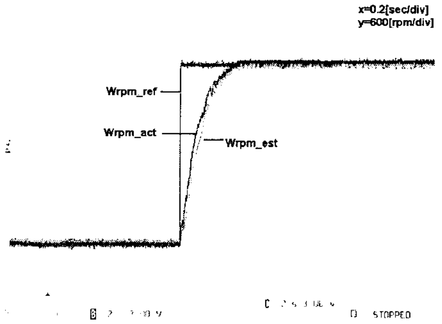

(b) Extended speed response in transient state
from -1500 to +1500rpm

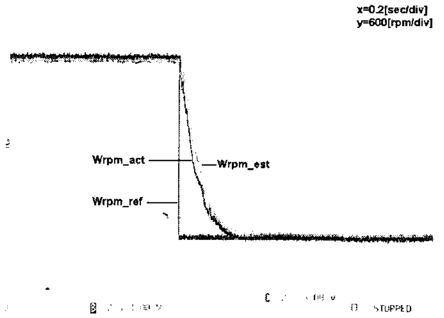

(c) Extended speed response in transient state
from +1500 to -1500rpm

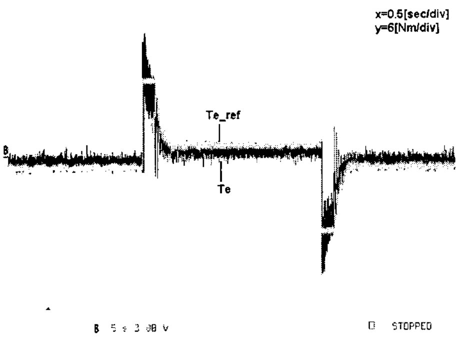

(d) Torque response characteristics

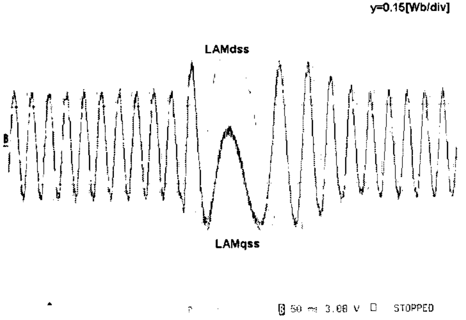

(e) Stator flux waveform in transient state

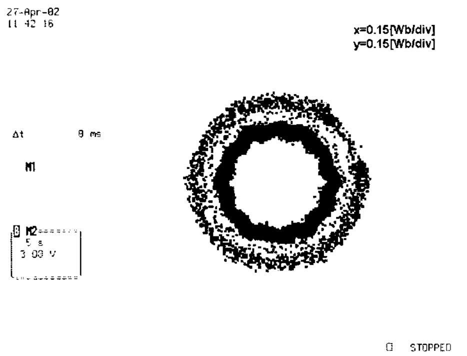

(f) Locus of stator flux

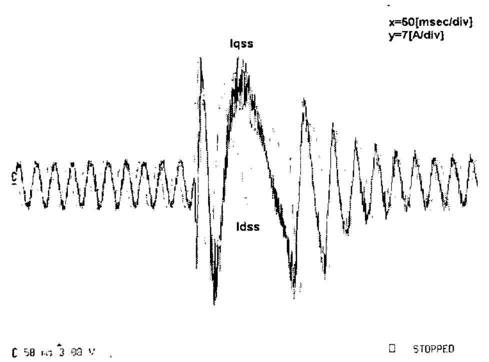

(g) Stator current waveform in transient state

Fig. 8. Experimental results at ±1500 [rpm]

Fig. 8 shows the experimental results for the response of speed control system during 5 seconds with a rotor speed ±1500 [rpm]. Fig. 8 (a) represents speed response characteristics, (b) and (c) extended speed response in transient state, (d) torque response, (e) stator flux waveform in transitent state, (f) locus of stator flux state, and (g) stator current waveform.

6. Conclusion

This paper presents preliminarily an implementation of digital sensorless speed control system for RSM drives with direct torque control by consideration of a nonlinearly inductances.

In order to prove the suggested sensorless speed control algorithm, we have a simulation and testing at actual experimental system. The developed sensorless control system show a good speed control response characteristic results and high-dynamic performance features in 20/1500 rpm with 1.0 kW RSM having 2.57 ratio of d/q reluctance. In this sensorless control system, there was no problem at high-speed range, but there were some torque pulsation and speed ripple at low speed range.

Acknowledgments

This work was supported by grant No. R02-000-00273 from the Basic Research Program of the Korea Science & Engineering Foundation.

References

[1] Takahashi and T. Noguchi, "A new quick response and high efficiency strategy of an induction motor", *in Conf. Rec. IEEE-IAS Annual Meeting*, pp. 495~502. 1985.

[2] M. Depenbrock, "Direct self control for high dynamics performance of inverter feed AC machines", *ETZ Arch.*, Vol. 7, No. 7, pp. 211~218, 1985.

[3] Min-Huei Kim, Nam-Hun Kim, Min-Ho Kim, and Dong-Hee Kim, “An Induction Motor Position Control System with Direct Torque Control”, *ISIE 2001*, pp. 771~774, June 2001.

[4] Min-Huei Kim, Nam-Hun Kim, and Won-Sik Baik, “A High-Performance Position Sensorless Control System of Reluctance Synchronous Motor with Direct Torque”, *Trans. of KIPE*, Vol. 7, No. 1, pp. 81~90, Feb. 2002.

[5] Min-Huei Kim, Nam-Hun Kim, and Kyeong-Ho Choi, “A

High-Performance Motion Control System of Synchronous Motor with Direct Torque Control", *Trans. of KIEE*, Vol. 51B, No. 3, pp. 150~157, March 2002.

[6] Kuo-Kai Shyu, Chiu-keng Lai, and John Y. Hung, "Totally Invariant State Feedback Controller for Position Control of Synchronous Reluctance Motor", *IEEE Trans. on IE*, Vol. 48, No. 3, pp. 615~624, June 2001.

[7] Matsuo, T. and Lipo, T.A., "Field oriented control of synchronous reluctance machine", *PESC '93 Record, 24th Annual IEEE*, pp. 425~431, 1993.

[8] Peter Vas, "Sensorless Vector and Direct Torque Control", *Oxford Press*, 1998.

[9] Iron Boldea, "Reluctance Synchronous Machines and Drives", Oxford Press. 1996.

[10] Bimal K. Bose, "Power Electronics and Variable Frequency Drivers", *IEEE Press*, 1997.

[11] Hoang Le-Huy, "Comparison of Field-Oriented Control and Direct Torque Control for Induction Motor", *PESC '99*, pp. 1245~1252, 1999.

[12] Jansen, P.L., R.D. Lorenz, and D.W. Novotny, "Observer-based direct field orientation in direct field oriented induction machines", *IEEE-IAS Annual Meeting*, pp. 536~543, Oct. 1993.

[13] Boldea I, Janosi L, and Blaabjerg F, "A modified direct torque control (DTC) of reluctance synchronous motor sensorless drive", *Electric Machines & Power Systems*, Vol. 28, No. 2, pp. 115~128, 2000.

[14] Alfio Consoli, Calogero Cavallaro, and Giuseppe Scarcella, "Sensorless Torque Control Syncrel Motor Drives", *IEEE Trans. on PE*, Vol. 15, No. 1, pp. 28~35, Jan. 2000.

Min-Huei Kim was born in Kyengbuk Province, Korea on August 25, 1951. He received the B.S. and the M.S. degree from Yeungnam University, Kyeungbuk, Korea, and Ph.D. degree from the University of Chung-Ang, Seoul, Korea, all in electrical engineering, in 1974, 1980, and 1989, respectively. He has worked the Research and Development for electric motor design of the Shinil Industrial Company from 1977 to 1978 in Seoul, Korea, In 1978, he joined an Instructor of the yeungnam Junior College, Daegu, Korea. He became an Assistant Professor, Associate Professor and Professor in 1981, 1987, 1992, respectively. From 1993 to 1995, he was a Visiting Research Professor in Power Electronics Application Center (PEAC) at The University of Tennessee, Knoxville, USA.

He is currently a professor in Department of Electrical Automatic Engineering at Yeungnam College of Science and Technology, Daegu, Korea. His research interests are a control system of motor drives, power converters, neural networks and it's application of power electronics. He is a member of the KIPE and JIEE, a life member of KIEE, and a senior member of IEEE.

Nam-Hun Kim was born in Donghae, Korea, in 1973. He received the B.S. degree in control and instrumentation engineering in 1998 from Samchok National University, Samchok, Korea and received M.S. degree in electrical engineering in 2000, from Yeungnam University, Daegu, Korea.

Currently, He is candidate for the Ph. D. in Yeungnam University. His interests include power electronics, and motor drives. He is a member of KIPE, KIEE, and student member of IEEE.

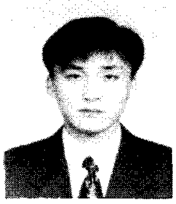

Won-Sik Baik was born in Daegu, Korea, on October 1970. He received the B.S. degree in Mathematics from Keimyung University, Daegu, Korea.

He is now working toward M.S. degree in Yeungnam University. His research interest is a control system of motor drives. He is a student member of KIPE and KIEE